Satellite Correlation between Aerosol Optical Depth and Cloud Optical Depth over Megacities

B. A. Sechrist[a] and Mark Z. Jacobson[ab], Stanford University, Stanford, CA, USA.

[a] Dept. of Civil and Environmental Engineering, Stanford University, Stanford, CA 94303, USA.
[b] jacobson@stanford.edu

Technical Report
Department of Civil and Environmental Engineering, Stanford University
December 31, 2017

Abstract

One of the most important remaining questions surrounding the impact of aerosol particles on climate is the extent to which they increase or decrease cloudiness upon an increase in aerosol loading. This issue has been examined in biomass burning regions of the Amazon but not in an urban area. This study begins to look at this question with MODIS-Aqua satellite retrievals of aerosol optical depth (AOD) and cloud optical depth (COD) over Los Angeles, New Delhi, and Beijing. Results suggest that, for Los Angeles, as AOD increased, COD generally decreased; for New Delhi, COD increased at low AOD and then decreased with increasing AOD; and for Beijing, COD remained approximately level as AOD increased. When the data retrievals were separated by season, the COD curve was either boomerang-shaped (increasing then decreasing COD as AOD increased) or decreasing for most city-seasons. Exceptions included New Delhi in autumn and Beijing in autumn and winter, for which COD remained nearly constant as AOD increased. These results generally support previous satellite and 3-D modeling results for biomass-burning regions of the Amazon that found boomerang-shaped relationships of COD versus AOD. However, the paucity of valid satellite retrievals suggests that the results here are of questionable statistical significance and much more work is needed to confirm them.

1. Introduction

Most every global and regional computer model of the impacts of aerosol particles on clouds and climate to date has assumed that cloud optical depth (COD) increases linearly with aerosol optical depth (AOD) (e.g., Myhre et al., 2013). At least one reason is that such models have considered only aerosol indirect and semi-direct effects, but not cloud absorption effects, of aerosol particles on clouds. The indirect and semi-direct effects don't capture cloud burnoff, which can occur at high aerosol loading due to cloud absorption effects (Jacobson, 2012). As such, most climate models may overestimate aerosol cooling, thus underestimate global warming resulting from aerosol feedbacks to clouds.

The aerosol *first indirect effect* is the increase in cloud aggregated cross-sectional area, thus reflectivity, due to the spreading of cloud water over an increased number of aerosol cloud condensation nuclei (CCN) (Twomey, 1977). The *second indirect effect* is the increase in cloud lifetime and time-averaged liquid water content and fractional cloudiness due to a decrease in cloud drop size and rainfall rate resulting from a higher aerosol loading (Gunn and Phillips, 1957; Albrecht, 1989).

The *semi-direct effect* is the decrease in cloud reflectivity due to the decrease in near-cloud relative humidity (RH) and increase in atmospheric stability caused by absorbing aerosol particles below, within, or above a cloud (Hansen et al., 1997; Ackerman et al., 2000; Jacobson, 2002; Koch and Del Genio, 2010; Bond et al., 2013). All studies of the semi-direct effect have assumed that black carbon (BC) and other absorbing aerosols are either externally mixed or internally mixed with the same coating (at the same RH) outside a cloud as inside the cloud.

Such an assumption, however, does not hold for aerosol particles within clouds, as aerosol particles interstitially between hydrometeor particles are at the RH of the cloud and swell and absorb more strongly by optical focusing than do aerosol particles within a cloud under the assumption that they are at the RH of the outside air. In fact, the transition between the ambient RH and the in-cloud RH that aerosol particles are affected by occurs within 0.5 km of a cloud (e.g., Flores et al., 2012). In addition, scattering by hydrometeor particles within a cloud enhances the exposure of interstitial absorbing aerosol particles to solar radiation, increasing absorbing aerosol heating more in a cloud compared with the clear sky (Jacobson, 2012).

More specifically, like swollen aerosol particles, hydrometeor particles containing absorbing aerosol inclusions absorb more sunlight than do aerosol particles without a coating due to optical focusing. Several studies have examined the potential effects of absorbing aerosol inclusions in hydrometeor particles. Danielson et al. (1969) calculated that such inclusions might explain partly why data indicate that thick clouds often have a low albedo. Absorption by inclusions in individual cloud drops has also been included in calculations of drop heating as a function of BC position in the drop (Chylek et al., 1996). Chuang et al. (2002), Sandu et al. (2005). Radiative forcing due to different BC volume fractions within liquid clouds has also been simulated (e.g., Erlick et al., 2006; Zhuang et al., 2010), as has global temperature change due to modeling radiative transfer through liquid and ice cloud particles with BC inclusions of different size (Jacobson, 2006, 2010).

The additional effects of absorbing aerosol particles at the relative humidity of the cloud on in-cloud heating are *cloud absorption effects* (CAEs) I and II. These are, respectively, the effects on cloud heating of both (I) absorption by aerosol inclusions within hydrometeor particles at the relative humidity of the cloud and (II) absorption by aerosol particles interstitially between hydrometeor particles at the in-cloud RH (Jacobson, 2012). CAE I and II are not part of the semi-direct effect, since the semi-direct effect has a specific historic definition and application that does not include CAE I or II. Whereas indirect effects usually enhance cloudiness, the combination of semi-direct and cloud absorption effects tends to burn off clouds (Kaufman et al., 2002; Kaufman et al., 2005; Kaufman and Koren, 2006; Rosenfeld et al., 2008; Ten Hoeve et al., 2012; Jacobson, 2012).

Several studies (e.g., Andreae et al., 2004; Kaufman and Nakajima, 1993; Koren et al., 2004; Koren et al., 2008; Ten Hoeve et al., 2011; 2012) have used satellite data to examine, by correlation, the net impact (thus the summed impacts of indirect, semi-direct, and cloud absorption effects) of aerosol particles on warm clouds over Rondonia, Brazil, during the biomass-burning season. These studies consistently found that the cloud optical depth (COD) – aerosol optical depth (AOD) relationship exhibits a "boomerang" shape in which COD initially increases with increasing AOD but then decreases as AOD continues to increase beyond some critical level. This result is thought to reflect the balance between the microphysical (indirect effects) and radiative (semi-direct and cloud absorption effects) components of a cloud's response to aerosols. The microphysical process dominates at low AOD, whereas the radiative

process dominates at high AOD. Ten Hoeve et al. (2012) subsequently showed by cause and effect (through 3-D modeling compared with data) the same boomerang curves over the Amazon found by satellite correlation.

Whereas the COD-AOD relationship has been probed extensively for biomass-burning regions, it has been examined only sparsely in other regions. Jacobson (2012) modeled the AOD-COD relationship on a global scale at course resolution, and Gradey et al. (2013) examined the AOD-cloud fraction relationship at a course global resolution. No study to date has examined the relationship at high resolution over urbanized regions. This study uses satellite data to examine this issue for Beijing, New Delhi, and Los Angeles, where the primary source of pollution is the combustion of fossil fuels or solid biofuels rather than open biomass.

These three megacities were chosen based on a combination of size, local meteorology, reputation for air quality, and potential impact on global climate. Los Angeles has a Mediterranean climate with cool, moderately rainy winters and warm, dry summers. Approximately 85% of precipitation occurs between December and March. New Delhi's climate is a cross between semi-arid and humid subtropical, with cool, dry winters and hot, wet summers. The climate's distinguishing feature is the monsoon season that runs from late June or early July to early October. The peak monsoon months of July and August are characterized by high humidity and copious amounts of rainfall, with approximately 60% of the annual rainfall occurring during July and August. Beijing has a humid continental climate with hot, humid, rainy summers and cold, relatively dry winters. Almost 75% of Beijing's precipitation occurs from June through August.

2. Data

Level 2 swath data from NASA's MODIS-*Aqua* satellite were collected for 1.5° x 1.5° regions encompassing the Los Angeles (33-34.5 N, 117-118.5 W), New Delhi (27.8-29.3 N, 76.4-77.9 E), and Beijing (38.7-40.2 N, 116-117.5 E) metropolitan areas. The 1.5° boxes were chosen to contain the city centers and major surrounding suburbs.

The data, from MODIS Collection 5.1, comprised daily satellite retrievals for one month (January, April, July, and October) during each of the four seasons over the years 2007 through 2012. MODIS Level

2 data are available at an output resolution of 10 km for aerosol properties, 5 km for cloud top properties, and 1 km for cloud optical properties. Because the resolutions of the raw outputs differ, the cloud top and cloud optical products were aggregated to match the 10 km x 10 km pixel size of the aerosol products. The cloud data were merged with the collocated aerosol data in preparation for analysis.

3. Methods

MODIS instruments generally cannot retrieve cloud and aerosol properties from the same area, but a 10-km output pixel contains 100 1-km input pixels, some of which are cloud free and used by the MODIS algorithms to compute representative aerosol properties for the 10-km region. Other 1-km pixels within the 10-km region contain cloud cover; these 1-km retrievals were averaged to yield the cloud properties for the 10-km region. The analysis was then conducted on the 10-km aggregates using the 10-km aerosol properties provided by NASA and the average 1-km cloud properties within each 10-km region.

Data from the MOD07 profile product, available at a resolution of 5 km, were also combined with the cloud and aerosol data to control for the effect of water vapor on the cloud-aerosol relationship. The analysis was performed on the 10-km aggregates. As in Ten Hoeve et al. (2011), observations were restricted to AOD below 0.8 to avoid aerosol misclassification as cloud.

Data quality is a major issue when working with satellite retrievals, and a tradeoff exists between the quantity and quality of the observations available for analysis. For each MODIS granule, NASA provides a quality assurance (QA) file to accompany the retrieved cloud and aerosol properties. The QA data can be used to screen the retrievals according to one's desired confidence level in the accuracy of the outputs. The analysis conducted here used both the unscreened outputs and those that were screened by the first ("marginal") level of confidence. QA screening that required "good" confidence in the data made the analysis impossible due to a lack of observations. The low confidence level in the accuracy of the retrieved data must be kept in mind when interpreting the results.

After the data were collected, the data for each region were pooled across all days during the period of study. The cloud fraction (CF) and COD of each output pixel were plotted versus the pixel's AOD. Next, the four seasons for which data were collected were examined separately to test whether or not seasonal differences in atmospheric conditions affected the cloud-aerosol relationship. The pixels were then

stratified according to their water vapor content, and the COD-AOD relationship was examined for different levels of water vapor in the column.

4. Results

The data were examined for correlations between the cloud and aerosol properties during each season, with a particular focus on the relationship between COD and AOD. Figure 1a shows all observations of co-located AOD and COD during the period of study. COD is binned by AOD, with each point representing the average COD within 12.5-percentile of the AOD value. This binning approach was used in Lin et al. (2006) and Ten Hoeve et al. (2011) for their studies of cloud-aerosol relationships. For Los Angeles, COD decreases with increasing AOD until AOD reaches approximately 0.2, after which COD remains approximately flat. For New Delhi, COD exhibits a boomerang shape in which it increases with AOD until AOD reaches 0.4 and then decreases with further increases in AOD. For Beijing, COD increases slightly at low AOD and then remains approximately flat as AOD continues to increase. Figure 1b displays the observations that remain after quality assurance (QA) screening. Only 12-25% of the original observations remain, depending on the city. With QA, the New Delhi COD-AOD curve loses its boomerang shape. The Los Angeles and Beijing curves retain their basic shape. Since aerosols can sometimes be misclassified as cloud, only AODs below 0.8 were included in the analysis (Brennan et al., 2005; Ten Hoeve et al., 2011).

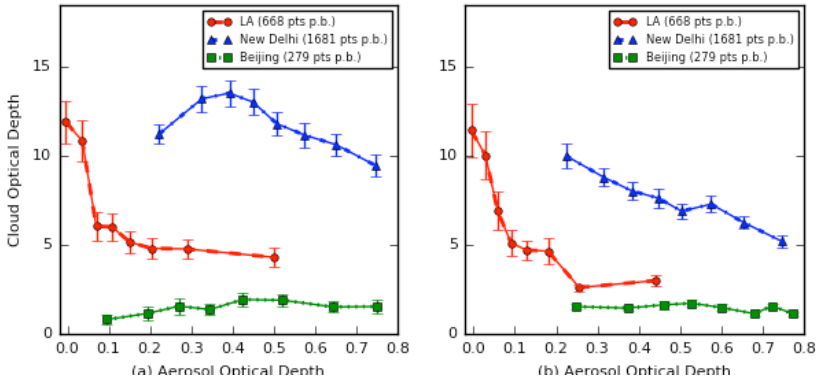

Figure 1. (left) Cloud optical depth binned by aerosol optical depth for all co-located retrievals over Los Angeles (red), New Delhi (blue), and Beijing (green) areas. Plotted data include all observations from the months of January, April, July, and October over the years 2007 through 2012. Error bars indicate 95% confidence intervals. (Right) Same as (left) but with quality assurance screening.

The six years of data were then separated by season. Figure 2 shows results for Los Angeles. Figure 2a indicates a decrease in COD with increasing AOD during January, and qualitatively (although not statistically) an increasing-then-decreasing trend during the other months. Figure 2b indicates that, depending on the season, between 24% and 33% of the original observations remain after quality screening. With QA, the same trends hold for January and July but not for April or October. Figure 2c shows that CF is flat to slightly increasing with increasing AOD for all months but January, in which CF increases with increasing AOD below an AOD of 0.1, but then decreases with increasing AOD thereafter. The error bars in Figure 2 are based on the observations in the sample and do not account for possible sampling bias due to retrieval failures.

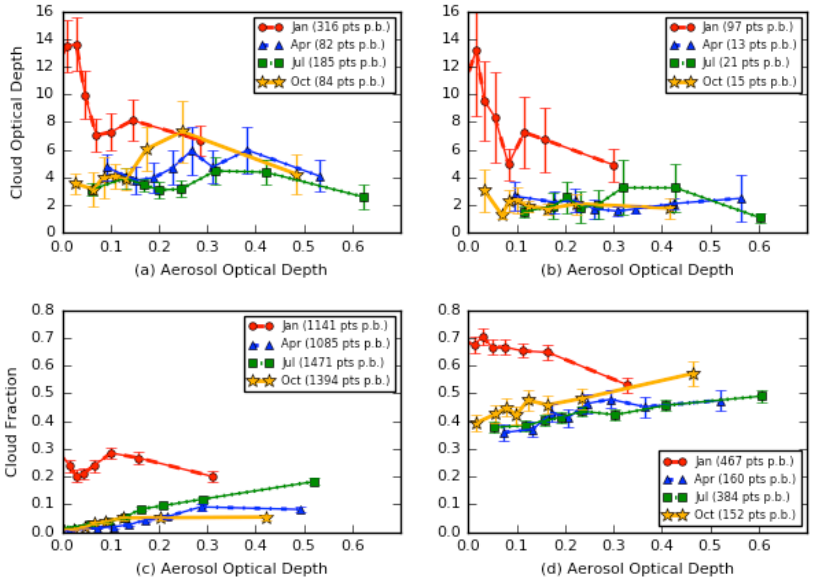

Figure 2. (a, top left) Los Angeles cloud optical depth binned by aerosol optical depth for all co-located retrievals during January (red), April (blue), July (green), and October (yellow) for the years 2007 through 2012. Error bars show 95% confidence intervals. (b, top right) Same as top left but with quality assurance screening. (c, bottom left) and (d, bottom right) Same as (a) and (b) but with cloud fraction on the vertical axis instead of cloud optical depth.

Figure 3 shows the same seasonal plots for New Delhi. The increasing-then-decreasing trend of COD with increasing AOD can be seen for all months in New Delhi except October. Fewer successful retrievals of AOD occur in July than in other months because of the presence of thick cloud cover associated with the summer monsoon during July. With quality screening (Figure 3b), the boomerang shapes of January and April are less pronounced but still present. Figure 3c indicates that in April, CF increases with increasing

AOD below ~0.45 and then decreases as AOD increases further. CF is approximately flat with increasing AOD during January and October. As with COD, fewer co-located observations of CF and AOD occur during July than other months because of the summer monsoon.

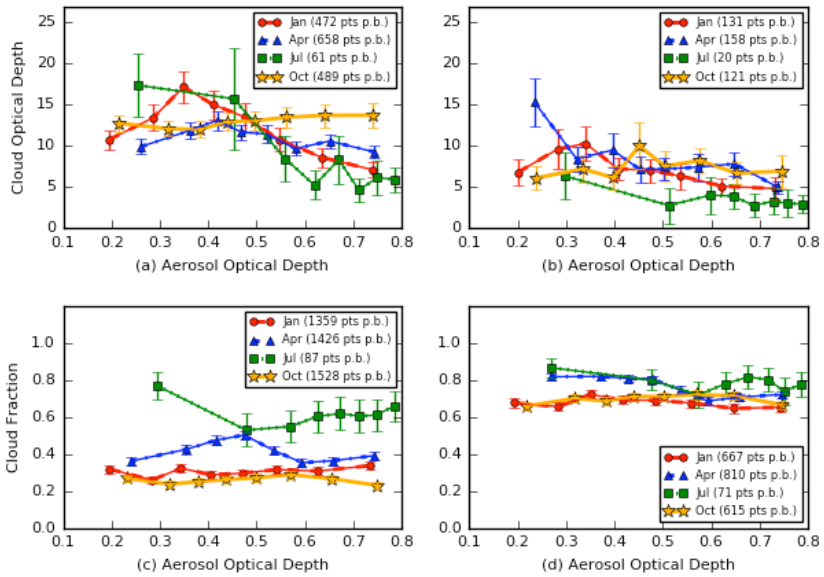

Figure 3. Same as Figure 2 but for New Delhi.

Figure 4 shows some qualitative evidence of an increasing-then-decreasing COD trend with increasing AOD for Beijing during January, April, and July. During October, COD is slightly flat or increasing with increasing AOD. Unlike with COD, CF appears to increase with increasing AOD during all seasons, although the increase is steepest during July.

Aerosols can sometimes be misclassified as cloud, so only AODs below 0.8 were considered in the analysis (Brennan et al., 2005; Ten Hoeve et al., 2011). Similarly, to make sure that cloud retrievals were really clouds, the data were re-analyzed with CODs only greater than 2.0. This restriction made little difference in the results. The retrievals were then categorized by water vapor content to investigate the effect of water vapor on the aerosol-cloud relationship. Data from the MOD07 profile product were merged with the cloud and aerosol properties, and the data were separated into top, middle, and bottom thirds by their water vapor content. The top and bottom thirds by water vapor content were then compared for each location and season. For no region did the COD-AOD relationship differ significantly between water vapor

levels. The data were also stratified by cloud fraction, but this yielded no insights beyond the seasonal analysis.

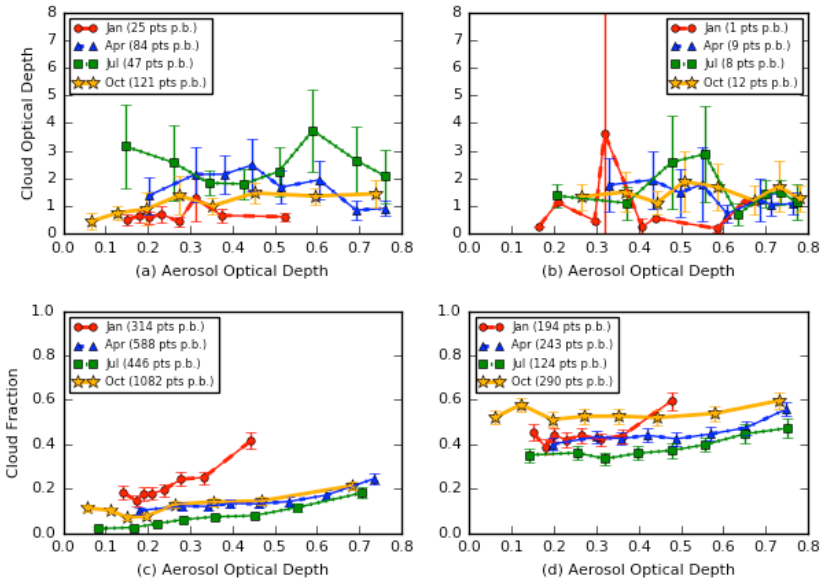

Figure 4. Same as Figure 2 but for Beijing.

Data quality is a problem when working with satellite retrievals. A major concern is the possibility that one property of interest affects the retrieval success rate or the values computed for another property of interest. For example, MODIS retrievals of aerosol properties are typically only successful for "cloud-free" pixels, meaning that areas with optically thick cloud cover might be underrepresented in the sample. The blue bars in Figure. 5 illustrate the distribution of CF for all pixels with co-located retrievals of CF and AOD in the Los Angeles area. These are overlaid on the distribution of CF for all successful retrievals of CF, illustrated by the red bars. For each month, there are far fewer retrievals of the co-located CF, and its distribution (blue) is skewed sharply toward lower values relative to the distribution (red) of all CF retrievals. This discrepancy suggests that pixels with high CF are underrepresented in the analysis.

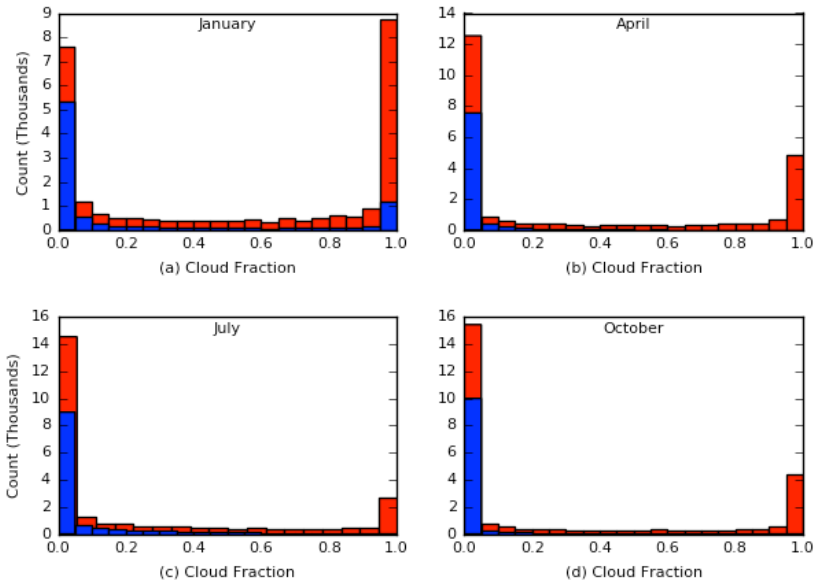

Figure 5. Los Angeles histogram of cloud fraction retrievals by month during the five year period of analysis. The red bars show the distribution of all cloud fraction retrievals. The blue bars show the distribution of cloud fraction retrievals for which there were successful co-located aerosol optical depth retrievals.

Figure 6 is similar to Figure 5 but for New Delhi. Compared with Los Angeles, the distribution of co-located retrievals for New Delhi is much closer to that of all CF retrievals. In other words, for New Delhi, the CF observations with co-located AODs are less skewed toward lower CF values. The exception is July, during which there were few successful retrievals of aerosol properties due to summer monsoon cloudiness. A similar analysis was conducted for Beijing. As with Los Angeles, the co-located distribution for Beijing shifted significantly toward lower CF relative to the full distribution. The similarity between the full and co-located distributions for New Delhi (July excepted) suggests that there may be less sampling bias for New Delhi than for Los Angeles or Beijing.

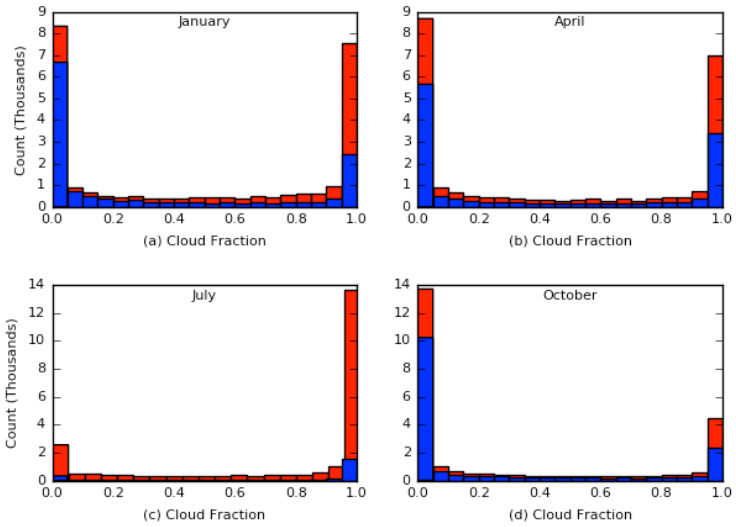

Figure 6. Same as Figure 5 but for New Delhi.

5. Discussion

Ten Hoeve et al. (2011; 2012) observed a "boomerang" relationship between COD and AOD for a region in the Amazon where the aerosols are primarily derived from biomass burning. Using a similar method, this study examined the COD-AOD relationship over three global megacities where the aerosols are largely generated by fossil-fuel combustion. When quality-screening procedures were not implemented, the COD-AOD relationship was observed to either decline or remain approximately constant at high aerosol concentrations. With quality screening, the size of the dataset was significantly reduced, and the COD-AOD relationship was often unclear. For both Los Angeles and Beijing during July, the boomerang curve still appeared to be intact with quality screening, but the small number of observations made it impossible to draw firm conclusions.

These results should be interpreted with several caveats in mind. The MODIS algorithms classify the AOD retrieval as successful for only about 6% of the 10-km pixels, and the success rate for COD (at 1-km resolution) is even lower. The spatial aggregation of a 1-km cloud property to 10 km might not accurately represent the cloud property in the 10 km x 10 km region if many of the 1-km retrievals are missing. Co-location of the clouds and aerosols in the vertical domain is also uncertain because the MODIS satellites carry passive sensors whose imagery lacks vertical resolution.

Any dependence of retrieval success rates on the properties of interest can bias the sample used in the analysis (Wilcox et al., 2009). The retrieval failures might be systematically related to the cloud-aerosol relationship; for example, MODIS retrievals of aerosol properties are typically only successful for "cloud-free" pixels, meaning that areas with optically thick cloud cover might be underrepresented in the sample. Furthermore, aerosol properties that are retrieved from pixels adjacent to clouds are subject to greater uncertainties.

6. Conclusions

Although there is significant uncertainty in the data quality, the results of this study generally corroborate the principal finding of Koren et al. (2004; 2008) and Ten Hoeve et al. (2011), namely a boomerang-shaped relationship between AOD and COD, but in this case for major urban areas (Beijing, New Delhi, and Los Angeles), where the dominant sources of pollution is the combustion of fossil fuels and, in the case of Beijing and New Delhi, biofuels. The agreement of these results suggests that the aerosol semi-direct effect plus cloud absorption effects have the potential to dominate aerosol indirect effects at high AOD across a range of aerosol types and atmospheric conditions. If this result holds true, then most models of regional and global climate, which almost all ignore cloud absorption effects, may overestimate the cooling feedback of aerosol particles to clouds, thus underestimate anthropogenic global warming. However, the poor sample size of quality data used here suggests that more work needs to be done to verify the results.

Acknowledgments
This study was supported by the NSF Atmospheric Chemistry Division (AGS-1441062) and the NASA Earth Science Division. The authors wish to thank J. E. Ten Hoeve for helpful input.

References

Ackerman A.S., O.B. Toon, D.E. Stevens, A.J. Heymsfield, V. Ramanathan, E.J. Welton (2000). Reduction of tropical cloudiness by soot, *Science, 288*, 1042-1047.

Albrecht, B. (1989). Aerosols, cloud microphysics, and fractional cloudiness, *Science*, 245, 1227-1230.

Andreae, M. O., Rosenfeld, D., Artaxo, P., Costa, A. A., Frank, G. P., Longo, K. M., & Silva-Dias, M. A. F. (2004). Smoking rain clouds over the Amazon. *Science*, *303*(5662), 1337-1342.

Bond, T.C., S.J. Doherty, D.W. Fahey, P.M. Forster, T. Berntsen, O. Boucher, B.J. DeAngelo, M.G. Flanner, S. Ghan, B. Karcher, D. Koch, S. Kinne, Y. Kondo, P.K. Quinn, M.C. Sarofim, M.G. Schultz, M. Schulz, C. Venkataraman, H. Zhang, S. Zhang, N. Bellouin, S.K. Guttikunda, P.K. Hopke, M.Z. Jacobson, J.W. Kaiser, Z. Klimont, U. Lohmann, J.P. Schwarz, D. Shindell, T. Storelvmo, S.G. Warren and C.S. Zender (2013), Bounding the role of black carbon in the climate system: A scientific assessment, *J. Geophys. Res.*, *118*, 5380-5552, doi: 10.1002/jgrd.50171.

Brennan, J. I., Kaufman, Y. J., Koren, I., & Li, R. R. (2005). Aerosol-cloud interaction-misclassification of MODIS clouds in heavy aerosol. *Geoscience and Remote Sensing, IEEE Transactions on*, *43*(4), 911.

Chuang, C.C., J.E. Penner, J.M. Prospero, K.E. Grant, G.H. Rau, and K. Kawamoto (2002), Cloud susceptibility and the first aerosol indirect forcing: Sensitivity to black carbon and aerosol concentrations, *J. Geophys. Res., 107*, 4564, doi:10.1029/2000JD000215.

Chylek, P., G.B. Lesins, G. Videen, J.G.D. Wong, R.G. Pinnick, D. Ngo, and J.D. Klett (1996), Black carbon and absorption of solar radiation by clouds, *J. Geophys. Res., 101*, 23,365-23,371.

Erlick, C., V. Ramaswamy, and L.M. Russell (2006), Differing regional responses to a perturbation in solar cloud absorption in the SKYHI general circulation model, J. *Geophys. Res., 111*, D06204, doi:10.1029/2005JD006491.

Flores, J.M., R.Z. Bar-Or, N. Bluvshtein, A. Abo-Riziq, A. Kostinski, S. Borrmann, I. Koren, and Y. Rudich (2012), Absorbing aerosols at high relative humidity: linking hygroscopic growth to optical properties, Atmos. Chem. Phys., 12, 5511-5521.

Grandey, B.S., S. Stier, and T.M. Wagner (2013) Investigating relationships between aerosol optical depth and cloud fraction using satellite, aerosol reanalysis, and general circulation model data, *Atmos. Chem. Phys., 13*, 3177-3184.

Gunn, R. and B.B. Phillips (1957) An experimental investigation of the effect of air pollution on the initiation of rain, *J. Meteorol.,* 14, 272-280.

Jacobson, M. Z. (2002) Control of fossil-fuel particulate black carbon plus organic matter, possibly the most effective method of slowing global warming, *J. Geophys. Res., 107* (D19), 4410, doi:10.1029/2001JD001376.

Jacobson, M.Z. (2006) Effects of externally-through-internally-mixed soot inclusions within clouds and precipitation on global climate, *J. Phys. Chem. A*, 110, 6860-6873.

Jacobson, M.Z (2010) Short-term effects of controlling fossil-fuel soot, biofuel soot and gases, and methane on climate, Arctic ice, and air pollution health, J. Geophys. Res., Atmospheres, 115, D14209.

Jacobson, M.Z. (2012) Investigating cloud absorption effects: Global absorption properties of black carbon, tar balls, and soil dust in clouds and aerosols, *J. Geophys. Res., 117*, D06205, doi:10.1029/2011JD017218.

Kaufman, Y. J., & Koren, I. (2006). Smoke and pollution aerosol effect on cloud cover. *Science*, *313*(5787), 655-658.

Kaufman, Y. J., Koren, I., Remer, L. A., Rosenfeld, D., & Rudich, Y. (2005). The effect of smoke, dust, and pollution aerosol on shallow cloud development over the Atlantic Ocean. *Proceedings of the National Academy of Sciences of the United States of America*, *102*(32), 11207-11212.

Kaufman, Y. J., & Nakajima, T. (1993). Effect of Amazon smoke on cloud microphysics and albedo: Analysis from satellite imagery.

Kaufman, Y. J., Tanré, D., & Boucher, O. (2002). A satellite view of aerosols in the climate system. *Nature*, *419*(6903), 215-223.

Koch, D., A. Del Genio (2010). Black carbon semi-direct effects on cloud cover, *Atmos. Chem. Phys*, 10, 7685-7696.

Koren, I., Y. Kaufman, L. Remer, J. Martins (2004). Measurement of the effect of Amazon smoke on inhibition of cloud formation, Science, 303, 1342-1345.

Koren, I., Martins, J. V., Remer, L. A., and Afargan, H (2008). Smoke invigoration versus inhibition of clouds over the Amazon, Science, 321, 946–949.

Lin, J. C., Matsui, T., Pielke, R. A., & Kummerow, C. (2006). Effects of biomass-burning-derived aerosols on precipitation and clouds in the Amazon Basin: A satellite-based empirical study. *Journal of Geophysical Research: Atmospheres*, *111*(D19).

Myhre, G., D. Shindell, F.-M. Breon, W. Collins, J. Fuglestvedt, J. Huang, D. Koch, J.-F. Lamarque, D. Lee, B. Mendoza, T. Nakajima, A. Robock, G. Stephens, T. Takemura, and H. Zhang (2013) Anthropogenic and Natural Radiative Forcing. In: *Climate Change 2013: The Physical Science Basis. Contribution of Working Group I to the Fifth Assessment Report of the Intergovernmental Panel on Climate Change* (Stocker, T.F., D. Qin, G.-K. Plattner, M. Tignor, S.K. Allen, J. Boschung, A. Nauels, Y. Xia, V. Bex and P.M. Midgley (eds.)). Cambridge University Press, Cambridge, United Kingdom and New York, NY, USA.

Rosenfeld, D., Lohmann, U., Raga, G. B., O'Dowd, C. D., Kulmala, M., Fuzzi, S., ... & Andreae, M. O. (2008). Flood or drought: how do aerosols affect precipitation?. *science*, *321*(5894), 1309-1313.

Sandu, I., P. Tulet, and J.-L. Brenguier (2005) Parameterization of the cloud droplet single scattering albedo based on aerosol chemical composition for LES modeling of boundary layer clouds, *Geophys. Res. Lett., 32*, L19814, doi:10.1029/2005GL023994

Ten Hoeve, J. E., Remer, L. A., & Jacobson, M. Z. (2011). Microphysical and radiative effects of aerosols on warm clouds during the Amazon biomass burning season as observed by MODIS: impacts of water vapor and land cover. Atmos. Chem. Phys, 11(7), 3021-3036.

Ten Hoeve, J.E., M.Z. Jacobson, and L. Remer (2012), Comparing results from a physical model with satellite and in situ observations to determine whether biomass burning aerosols over the Amazon brighten or burn off clouds, *J. Geophys. Res.*, *117*, D08203, doi:10.1029/2011JD016856.

Twomey, S. (1977). The influence of pollution on the shortwave albedo of clouds, *J. Atmos. Sci.*, 34(7), 1149-1152.

Wilcox, E. M., Harshvardhan, & Platnick, S. (2009). Estimate of the impact of absorbing aerosol over cloud on the MODIS retrievals of cloud optical thickness and effective radius using two independent retrievals of liquid water path. *Journal of Geophysical Research: Atmospheres (1984–2012)*, *114*(D5).

Zhuang, B.L., L. Liu, F.H. Shen, T.J. Wang, and Y. Han (2010) Semidirect radiative forcing of internal mixed black carbon cloud droplet and its regional climatic effect over China, J. *Geophys. Res., 115*, D00K19.